Article:
Dhimish, Mahmoud, Ahmad, Ameer and Tyrrell, Andy (2022) Inequalities in photovoltaics modules reliability: From packaging to PV installation site. Renewable Energy. pp. 805-814. ISSN: 0960-1481

https://doi.org/10.1016/j.renene.2022.04.156

Inequalities in Photovoltaics Modules Reliability: From Packaging to PV Installation Site

Mahmoud Dhimish*[1], Ameer Ahmad[2] and Andy M. Tyrrell[1]

[1] Department of Electronic Engineering, University of York, York YO10 5DD, UK

[2] Alsuwaidi F T S Building Construction L.L.C, Dubai, United Arab Emirates

*Corresponding Author: M. Dhimish (Mahmoud.dhimish@york.ac.uk)

Abstract

In recent years, the determination of the reliability of photovoltaic (PV) modules has been of ubiquitous interest to the PV industry. Therefore, this work reports on the reliability and degradation mechanism of 186 PV modules from packaging to installation stage. The paper shows that no cracks or hotspots affecting the PV modules before the packaging stage, while a minor reduction in the output power was observed at ±0.3%. The same PV modules were delivered using standard practice, and no further precautions were considered. Electroluminescent (EL) images of all PV modules were taken at the PV installation site, and it was discovered that 2.2% evolved cracks. Depending on the crack size, the estimated output power losses under standard test conditions varied from 0.53% to 1.43%. Furthermore, the PV modules were thermally inspected six months after being installed. It was found that hotspots developed in all the cracked PV modules, and their temperature increased from 10°C to 20°C. In addition, a potential induced degradation (PID) test was performed on the cracked PV modules and compared with a crack-free module. It was found that PID affected the modules with cracks more than the crack-free module.

Keywords: Solar cells; cracks, electroluminescence, performance analysis, potential induced degradation.

1. Introduction

One of the most valuable attributes of solar cell technology is its high stability, with operational lifetimes of over 30 years. Nevertheless, there are numerous degradation mechanisms, and these collectively reduce the module output power over time. One of the main degradation mechanisms is called potential-inducted-degradation (PID) [1, 2]. For many photovoltaic (PV) systems, PID is one of the leading causes of module degradation and is caused by voltage and the interaction of this stress factor with temperature and humidity. Recent studies prove that PID could develop due to pre-existing cracks or hotspots developed in the PV modules during their manufacturing and packaging/shipment procedures. Therefore, according to the current IEC/TS60904-13 [3], PV modules are advised to be inspected using an electroluminescence (EL) imaging setup or at least thermally when they arrive at the PV site before they are mounted/installed.

Several stages are passing during the production of PV modules. However, it was demonstrated that cracks could develop during the assembly of solar cells into full-scale PV modules [4]. PV cracks could be as small as micro-level or inactive/breakdown areas in the solar cells (Figure. 1) [5]. In contrast, there is no published information regarding the output power losses of the PV modules before and after being transported to the PV installation site.

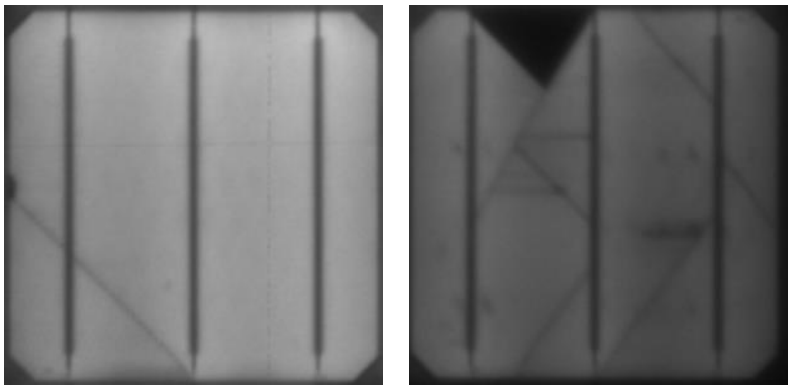

(b) (a)

Figure 1. Solar cells affected by cracks or structural defects. (a) Micro-crack, (b) micro-cracks and breakdown area (represented by the black area) [5].

In a recent study, [6], a PV module subjected to a reverse bias of 160 V was shown to exhibit severe PID, leading to the formation of hotspots which appeared on the modules. This study showed that the PID resulted in a reduction of the current density and the open-circuit voltage. Improved testing has been the focus of much recent research; for example, in [7], the authors have presented an approach to examining different types of cracks in bifacial passivated emitter rear contact (PERC) solar cells.

Other researchers [8, 9] have reported that cracks in solar cells can accelerate the PID effect due to the localized heat caused by the cracks. This work was supported by studies conducted using electroluminescence (EL) imaging before and after PID testing. This affirmed that cracks could lead to hotspots in the solar cells, and as a result, PID is expected, yet there were no discussions on the type/size of cracks and their anticipated impact on PID.

To prevent PID or cracks in solar cell level, an optimization for the antireflection coating (ARC) must be determined [10-12]. These recent studies show that the thin silicon dioxide (SiO_2) ARC layer combined with n-type and p-type solar cells can reduce the number of solar cells that experience PID. However, this coating layer cannot prevent cracks and structural defects, resulting in a PID for that solar cell.

At a PV module level, comprising 30 or more solar cells connected in strings, every component in the PV must be PID resistant [13, 14], including the encapsulants, absorption layers, and preferably the glass, as small leakage currents can cause ion migration. In addition, there are currently no mitigation techniques developed to overcome cracking in solar cells. In contrast, since 2015, there have been a number of attempts to create suitable devices to mitigate PV hotspots, such as those implemented using power electronics circuits [15-17]. These devices are executed to replace previously commonly used bypass diodes alliance with PV modules. However, they are not yet commercially available or at least experimented with large scale PV systems.

Therefore, these mismatched conditions affecting PV modules will likely lead to significant output power losses and levelized degradation rates. Consequently, it is important to investigate whether cracks can develop before the PV modules are installed at the PV site. This interpretation would also give us an unknown upshot on the reality of the PV production and packaging/shipment process overall. Accordingly, this paper demonstrates the results of examining the output power losses, hotspots, cracking modes, and PID of 186 PV modules as soon as they are assembled during the PV manufacturing process and at the PV installation site.

This paper is organized as follows: Section 2 comprises the sample preparation, the description of the EL testing setup, and output power loss estimation before the packaging/shipment phase. Section 3 presents the results of the examined PV modules after being arrived at the PV installation site. Section 4 shows the PID testing of the PV modules, whilst the conclusions of the complete study are presented in Section 5.

2. Samples Preparation and Experimental Procedure: Before Shipment/Packaging

2.1 PV Manufacturing Process

The solar cells production/fabrication line is shown in Figures. 2(a) and 2(b) with over 300 cells/day pipeline production capacity. The manufactured solar cells are crystalline silicon (c-Si), and the cells' main electrical and physical parameters are,

- Short circuit current density J_{sc} is equal to 38.8 mA/cm^2.
- Open-circuit voltage V_{oc} is equal to 0.61 V.
- Peak power at maximum power point is 3.685 W.
- The solar cells are made of three busbars.
- Conversion efficiency of 17.4%.

A full-scale PV module (Figure. 2(c)) is then assembled using 60 series-connected solar cells, providing a total of 221.1 W output power at standard test conditions (solar irradiance 1000 W/m^2, when the PV module and cells are at standard ambient temperature of temperature 25°C with sea level air mass (AM) of 1.5 (1 sun)).

(a) (b)

(c)

Figure 2. (a) Solar cell manufacturing line, (b) Solar cells ready to be assembled into full-scale PV module, (c) Full-scale PV module after production is completed.

2.2 Electroluminescence Imaging

Initially, EL imaging setup (Figure. 3(a)) has been used, the EL camera is provided by BrightSpot Automation. The EL comprises a digital single-lens reflex camera with a resolution of $6k \times 4k$ pixels, and the filter is removed and calibrated to allow sensitivity to electroluminescence picture (peak wavelength 1150nm) [18, 19]. The camera lens is 18-55 mm, and a programmable 15 A, 60 V power supply is available to connect with the PV modules.

The EL imaging provides a detailed picture of how healthy the solar cells have been assembled into full-scale PV modules that, in practice, are ready for the output power testing phase. For example, Figure. 3(b) presents the EL image of two examined PV modules. There are no cracking or breakdown regions observable in either PV sample. The dots and points (dark areas in some solar cells) represent healthy solar cells; these usually develop due to the low radiative recombination of carriers when completing the EL test.

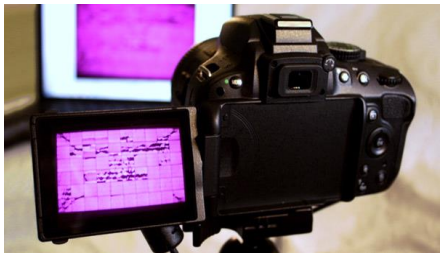

(a)

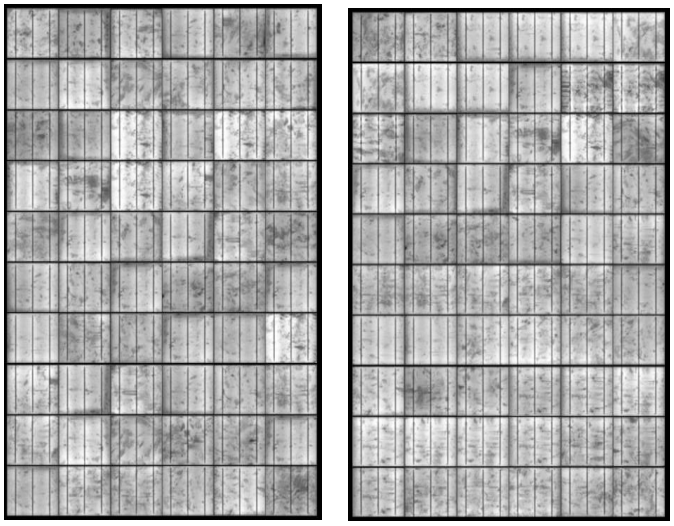

(b)

Figure 3. (a) EL imaging setup, (b) Example of EL images for two examined PV modules.

2.3 Output Power Loss Estimation

A PV simulator (SPI-Sun Simulator 4600SLP) was used to measure the PV modules' output power and control the relevant parameters (sun simulation and temperature). The output power loss is determined using (1), where P_{ref} is the output measured power of the reference PV module (221.1 W, theoretical maximum output power), and the P_{sample} is the output measured power for the tested PV module.

$$Output\ Power\ Loss\ (\%) = \frac{P_{ref} - P_{sample}}{P_{ref}} \times 100 \quad (1)$$

An irradiance and temperature cycle must be performed following the IEC61215 standard for testing PV modules after their production is complete. This step is required to guarantee PV modules are reliable and their current-voltage (I-V) and power-voltage (P-V) curves are accurately detailed in the manufacturer datasheet. During this experiment, it is expected to observe a minimal reduction in the output power. If the output power is reduced by 2% or more, the PV module fails the test and is recycled.

The testing procedure has the below Sun and temperature cycle, the temperature is measured in Celsius and 1 Sun is equivalent to 1000 W/m^2,

1) Sun cycle 1: 0.1, 0.5, 1.
2) Sun cycle 2: 0.1, 0.5, 1.
3) Temperature cycle 1: 30, 5, 50
4) Temperature cycle 2: 30, 5, 50

This procedure has been performed on a pack of 186 PV modules. The output of the Sun and temperature cycles against output power losses are presented in Figure. 4. According to the Sun cycles (Figure. 4(a)), the output power loss slightly decreases as the sun level increase. The maximum output power loss is 0.27% for a 0.5 Sun level. In contrast, there are nearly identical output power losses during the temperature cycles (Figure. 4(b)). The maximum output power loss is 0.23% at 50°C.

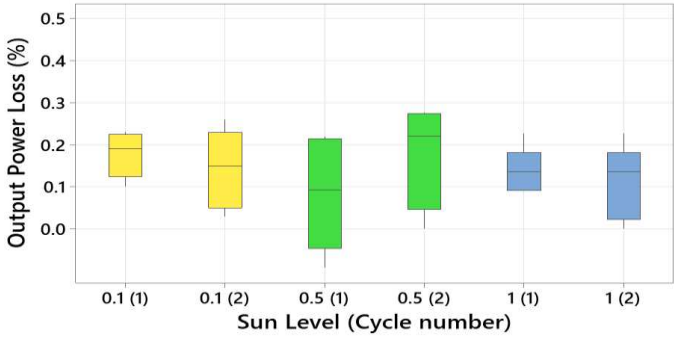

(a)

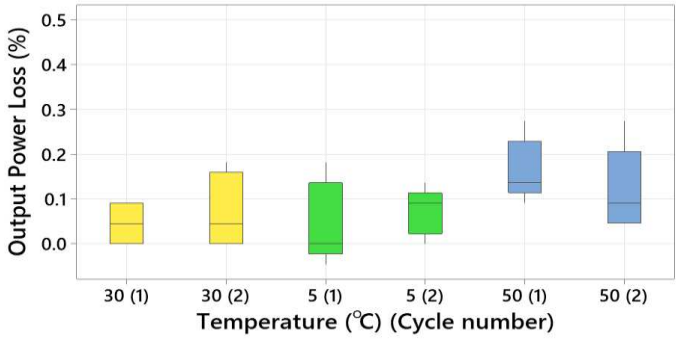

(b)

Figure 4. Performance of the PV modules before packaging/shipment. (a) Output power loss at varying Sun levels, (b) Output power loss at varying temperatures.

These results confirm minimum power losses in the PV modules, and therefore, at STC conditions the new reported maximum output power is 219.34±0.66 W. In addition, in Figure. 5, illustrates the averaged I-V and P-V curves for all PV samples.

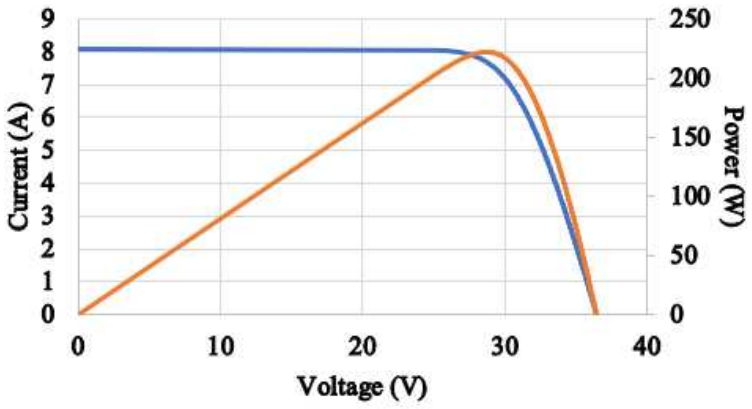

Figure 5. I-V and P-V curves of the manufactured PV modules are taken after performing the Sun and temperature cycles under STC conditions.

Before discussing the shipping/packaging process, there are several outcomes from these conduct tests to be highlighted:

1) After completing solar cells manufacturing and PV-scale assembling, no cracks or breakdowns were observed for all PV module samples.
2) The output power is slightly adjusted (from 220 into 219.34±0.66 W) after completing the Sun and temperature cycles testing procedure.
3) There was no overheating or what is known by hotspots detected for all the considered PV modules.

3. Experimental Procedure: After Shipment/Packaging Process is Completed

3.1 Shipment/Packaging Procedure

The PV modules were packed and transported to the installation site in six pallets, and every pallet contained 31 PV modules (Figure. 6(a)). Therefore, 186 PV modules with a maximum PV site capacity of 40.92 kW. This process was managed with careful consideration using a courier delivery (Figure. 6(b)). The site is located 10 miles away from the actual PV manufacturer (Changsha District, China). The complete PV setup after being installed is shown in Figure 6(c).

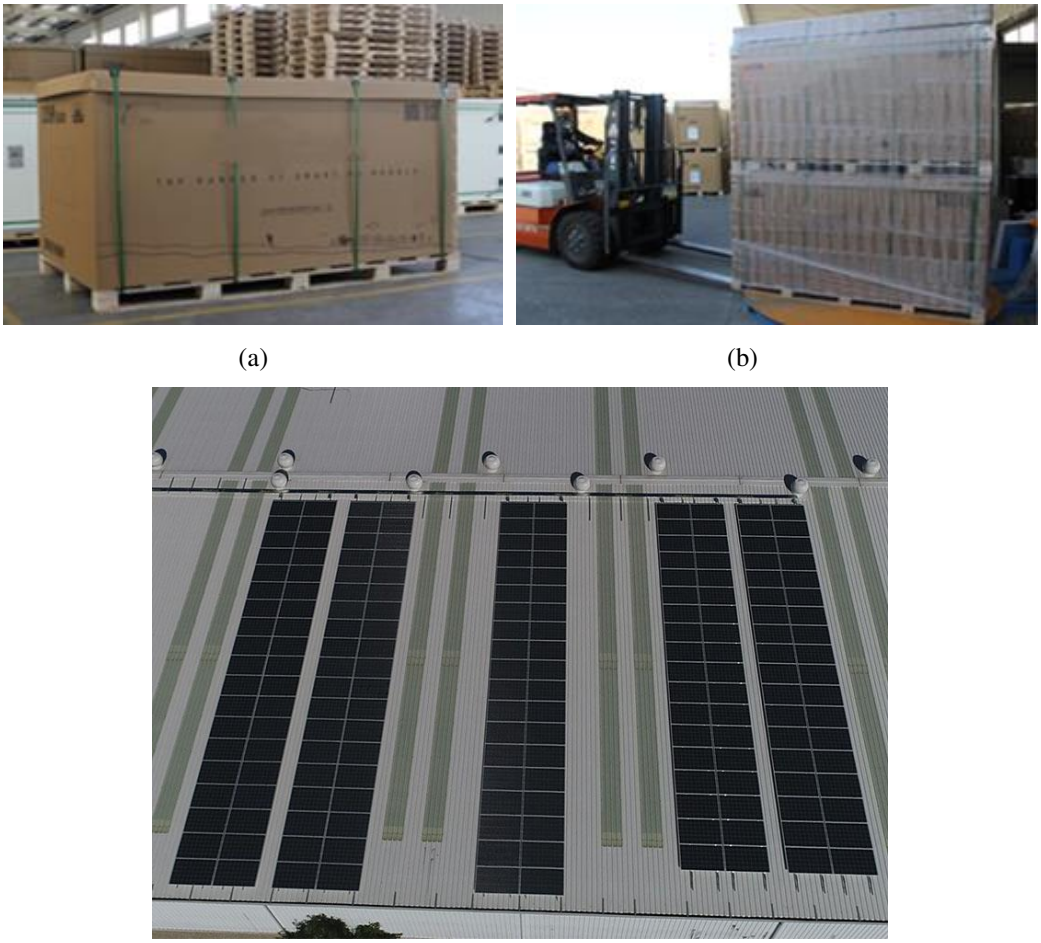

(a) (b)

(c)

Figure 6. (a) Pallet of PV modules, this pallet contains 31 PV modules, (b) Forklift handling two pallets simultaneously; this picture was taken during the transport phase of the PV modules from the PV manufacturer to the installation site, (c) PV site after the models were installed.

3.2 Field Electroluminescence imaging – Cracking modes

After receiving the PV modules at the installation site, another EL test was performed following the IEC/TS60904-13 [3]. Four PV modules have been affected by different cracking modes (2.2% of the total PV modules) appeared after transportation. After being installed, the complete PV setup is shown in Figure 6(c).

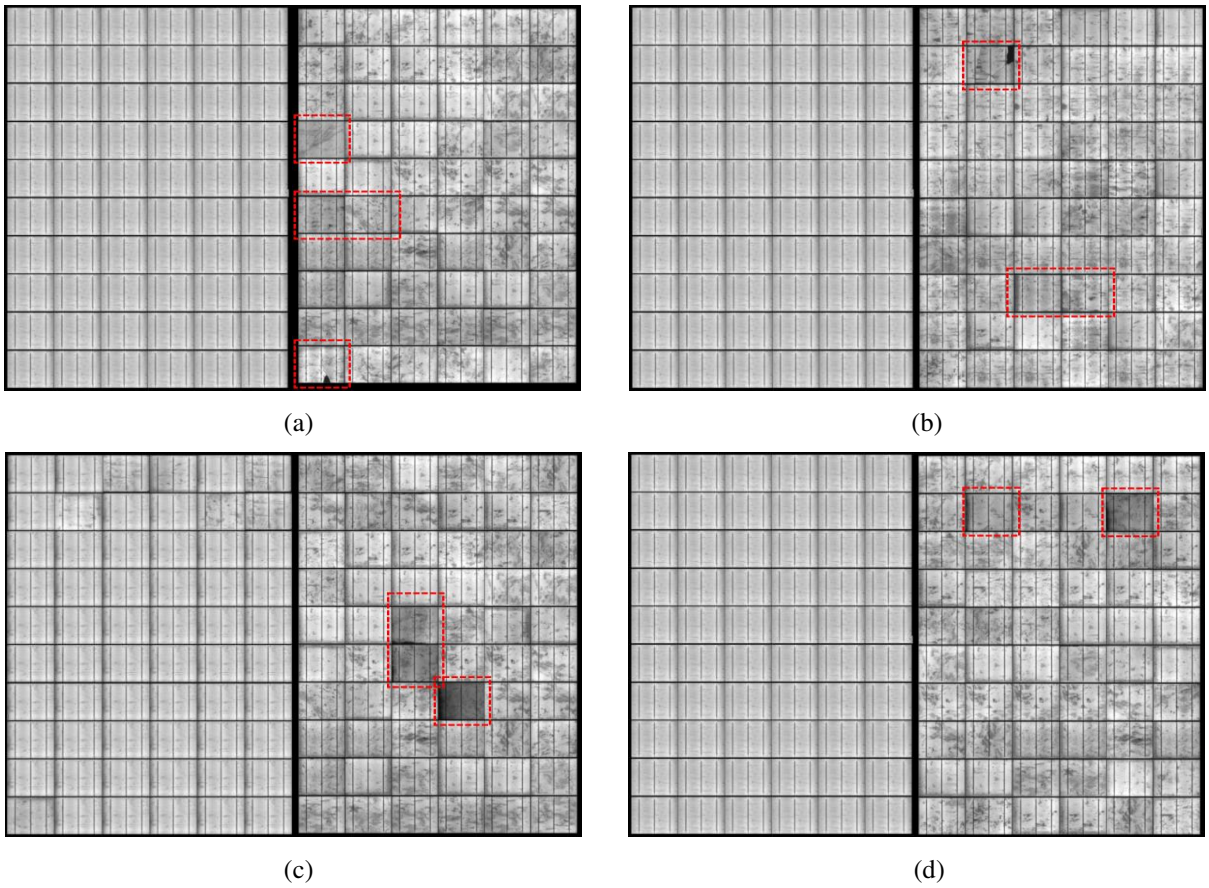

Figure 7. EL images before and after shipment for the cracked PV modules. (a) PV module #1, (b) PV module #2, (c) PV module #3, (d) PV module #4.

Three solar cells in the middle of the first PV module have micro-cracks (Figure. 7(a)). In addition, the EL image shows a breakdown area on the bottom edge cell. The same observation is seen in PV module #2 (Figure. 7(b)). It is not usual to observe micro-cracks in modules, as packing/unpacking PV modules can usually result in minor defects. However, the breakdown regions representing a complete in-active area often happen after PID. The modules are new to the site and have not been exposed to environmental conditions. Therefore, it is unlikely that these defects in the cells are due to PID or prior testing. Thus, the valid reasons that these breakdown regions are transpired in the modules during the transportation phase.

PV modules #3 and #4 have partially shaded solar cells but with no observed micro-cracks or breakdown regions. From previous research [20-22], it is understood that these cells can be inactive after PID affects the PV modules. In addition, these cells are also most likely to develop hotspots. This will be discussed further in the next section.

To investigate the additional power losses caused by the cracks, the PV modules were tested using the SPI-Sun solar simulator under STC conditions; the results are shown in Figure. 8. The modules are dismounted from the PV array and tested with a sun simulator. A professional engineer has carefully handled this testing stage. There is no alternative procedure to test the modules under STC conditions other than following this strategy. These tests might have created a new cracked, but, evidenced from the EL images in Figure 7, the cracks already existed, and the power losses are also predictable.

The output power losses range from 0.53% to 1.43%. The output power loss is significantly more than the output power loss boundary taken before shipment/packaging (highest at 0.27% in Figure. 4). This suggests that a permanent reduction in the output power of these PV modules is warranted, and the PV modules reliability has been obstructed.

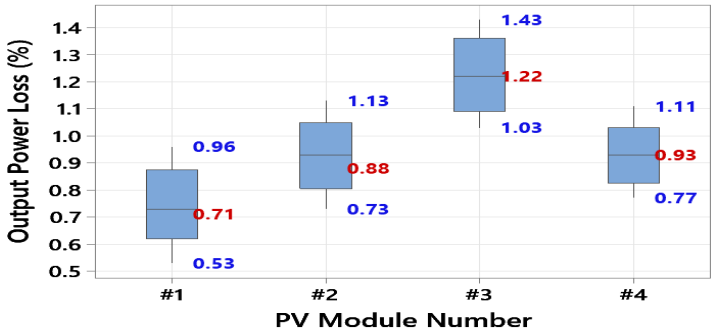

Figure 8. The output power loss of the PV modules (#1 - #4) under STC conditions.

3.3 PV Hotspots development

For PV hotspots to develop, the good practice is to inspect the PV modules after a couple of months of field operation. For example, Figure. 9 shows the thermal image of the PV module #1 taken at 693 W/m^2 and a PV cell temperature of 21.7°C. It is clear that there is no alleviation of the cell's temperature (no hotspots).

following these resulls, the PV modules were thermall examined after 6-months of field operations (Figure. 10) taken under solar irradiance of 772 W/m^2 and cell temperature of 23.3°C. The thermal images were captured using FLIR E75 (thermal sensitivity ±0.1°C) and calibrated using FLIR software.

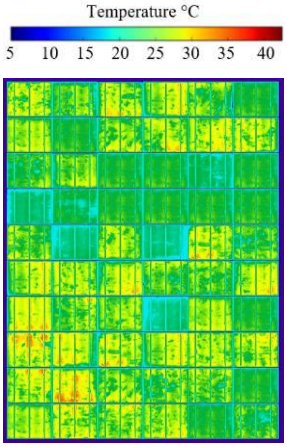

Figure 9. Thermal image of PV module #1 before field operation (no presence of hotspots).

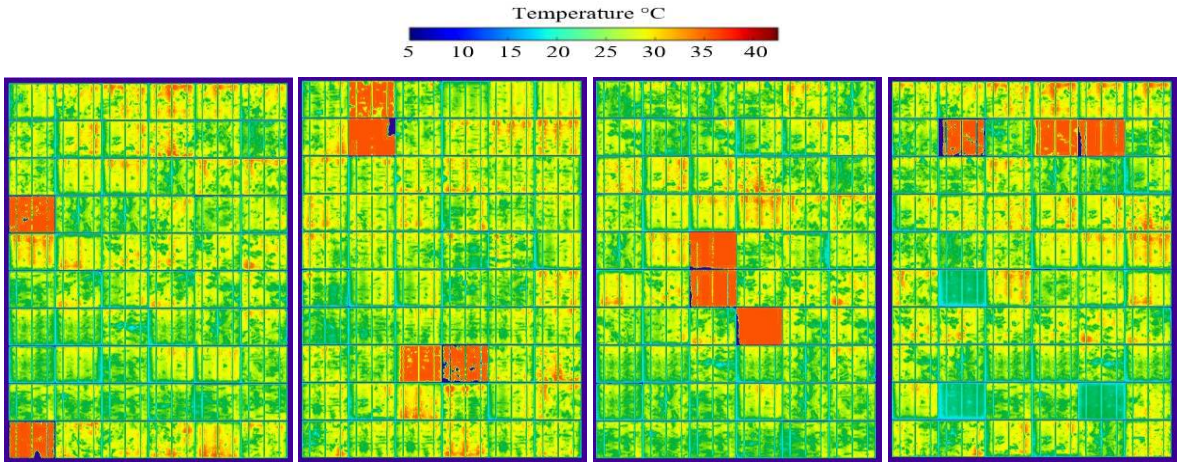

(a) (b) (c) (d)

Figure 10. Thermal images of the cracked PV modules after 6-months of field operation, taken under solar irradiance 772 W/m^2 and cell temperature 23.3°C. (a) PV module #1, (b) PV module #2, (c) PV module #3, (d) PV module #4.

As expected, the cracked PV modules are now exhibiting severe hotspots. The hotspots temperature varies from 35°C to nearly 40°C, compared with non-hotspot cells at approximately 23.5°C. Furthermore, the location of the hotspots is identical to the cracked cells in the original EL images shown in Figure. 7. The cracks in the PV modules can act as an inactive region (permanent shade). Consequently, the hotspots developed in a relatively short period. As developed by [15, 23], these methods proposed suitable techniques to recover PV hotspots by replacing the bypass diodes with power electronics devices, yet the hotspots themselves are challenging to mitigate completely.

A Solmetric PVA-1000S PV analyzer has been used to record the output I-V curves (Figure. 11) under solar irradiance of 772 W/m^2 and cell temperature of 23.3°C. During the test, an overcasting condition in the sky explains the step change in the I-V curves. The accuracy for the PV analyzer is ±5%. It is observed that the PV modules have a power loss ranging from 0.77±5% to 1.44±5% compared with an adjacent PV reference module (a healthy PV module with no cracks or hotspots). The maximum decrease in the short circuit current is equal to 0.2 A, and no significant difference in the open-circuit voltage (approximately 0.07 V).

In Figure 11, it can be observed that the power losses of the PV modules are not exactly consistent with the development of the hotspot in the modules. For example, even though PV module #2 has four hotspots, its power loss is less than PV module #3, which has three hotspots. There are two reasons behind this behaviour, (i) the hotspots in PV module #3 have a higher temperature increase compared with the PV module #2, (ii) the development of the hotspot is not necessarily a sign of the impact of the actual crack on the modules; hence, EL imaging can illustrate the differences between the crack sizes and breakdown in the cells, while the thermal image can only show the increase of the surface temperature.

As the PV modules are still in the first year of operation, it could be concluded that the PV modules' degradation rate is the same as the power losses, averaged at 1.03±5%. Usually, this is not a considerable degradation rate of PV modules in their first year. Yet, it is expected that due to the cracking, the PV modules will result in a further increase in the hotspots temperature and a significant degradation rate in the near future. Therefore, an excellent exercise to replace those with newer PV modules.

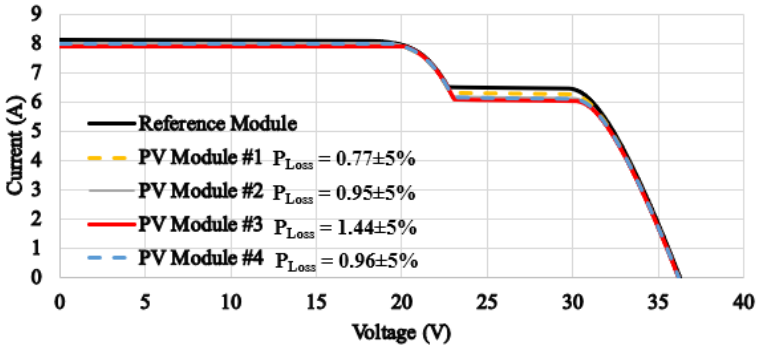

Figure 11. Output I-V curve taken for the hotspotted PV modules under solar irradiance 772 W/m^2 and cell temperature 23.3˚C.

4. PID Testing

If the cracked PV modules were left under field operation, PID likely affects them due to cracks and hotspots. Therefore, the cracked PV modules were dismounted and a PID test performed. For comparative investigation, the PID test on the healthy PV module were also completed. Following the IEC/TS60904-13 PID-testing standard, the examined PV modules were subjected to a temperature of 60°C with 80% humidity and under 1000 V load for 96 hours. The EL images before and after the PID test was completed are shown in Figure 12.

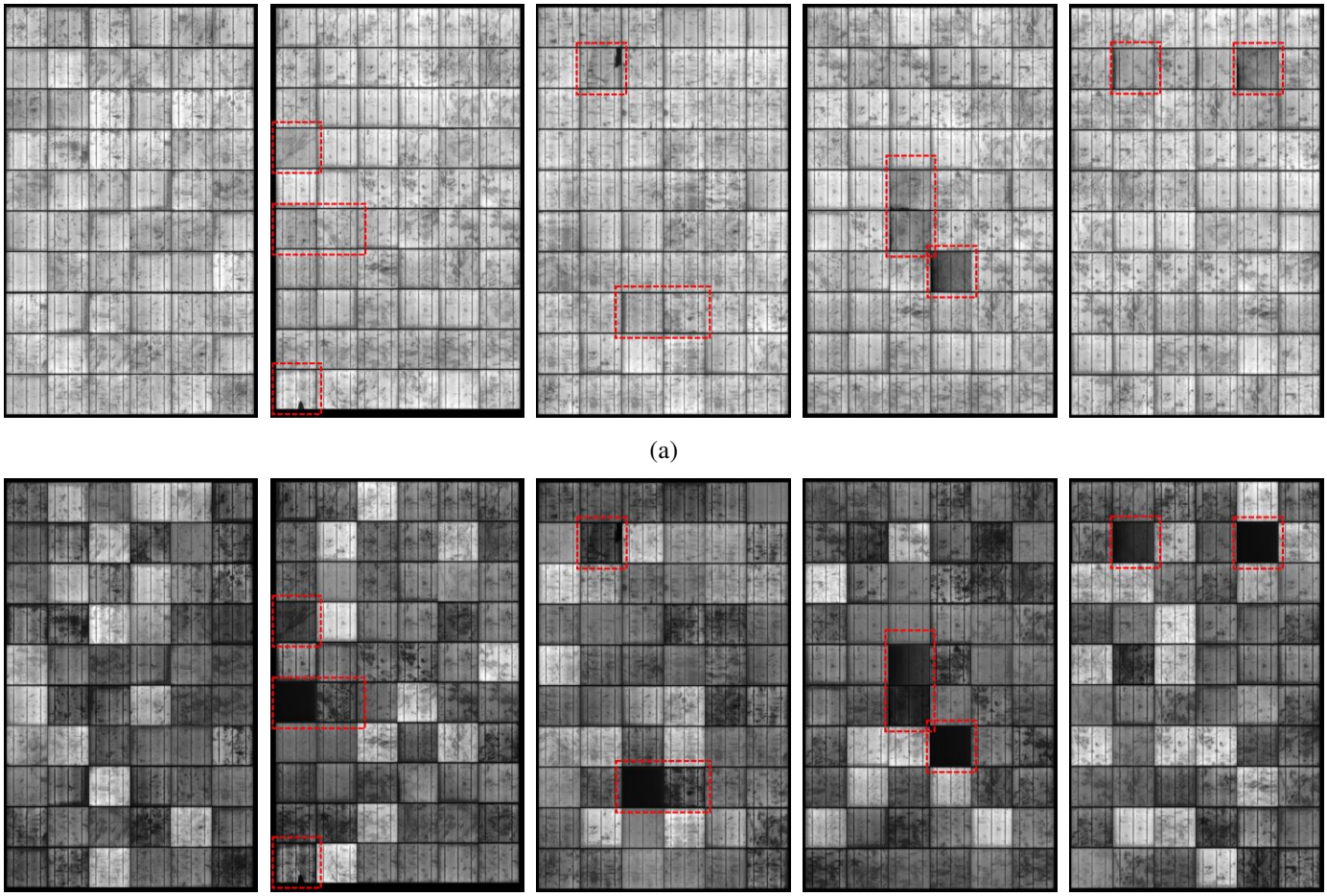

(a)

(b)

Figure 12. EL images of the examined PV modules samples. (a) Before the PID test, (b) After the PID test is completed. In this figure, from left to right, the first EL image is for the reference module (crack-free and with no power losses), followed by PV#1, PV#2, PV#3, and PV#4 which are already affected by cracks, even before the PID test started.

In practice, the PID forms in PV strings in two different settings, but both are attributed to the inverter or power electronic device having no grounding. First, it creates either +1000 V or -1000 V biasing for the affected PV string. The PID will then cause the PV modules to leak the current from the semiconducting material to the actual framing or glass [26]. Consequently, it will degrade the modules and cause a considerable drop in the output power production [27].

Prior work on PID has considered testing the PV modules under a controlled environment by applying the existing PID testing procedure: humidity 85%, PV surface temperature at 65℃ and bias of the PV module with either +1000 V or -1000 V, for at least 96 hours [27-29]. This test can, of course, lead to an understanding as to how PID can affect the PV modules. For example, in [30], it was shown that PID could reduce the module's output power by more than 30%. However, there is currently little information on whether the same percentage of power losses would result from PID under outdoor field conditions. In addition, it is unidentified if repairing the grounding issue of the affected PID strings would result in an increase in the output power and improve the quality of the affected modules. Finally, from [27, 31], through electroluminescence (EL) imaging, PID can cause shunting, cracks, and breakdown areas at a solar cell level [32].

In this paper, the output EL images after the PID test show that full breakdown solar cells (expressed by blacked cells) have only been exhibited for the PV modules where cracks have already formed. This outcome supports previous conclusions, as cracked solar cells are likely to impact PV modules with a significant degradation rate.

Previous research [24, 25], has suggested that the PID test can result in a nearly 20-30% drop in the output power, even for healthy PV modules. For the examined PV modules, the comparison between the output power loss at STC conditions before and after the PID test is shown in Figure 13, using an I-V curve illustration. All the electrical parameters results are also summarised in Table 1.

Before the PID test, the maximum output power loss was observed for the third PV module at 1.36%, compared with the reference PV module. However, after the PID test, there was a significant drop in the output power of the cracked modules compared with the healthy/reference module. For example, the third PV module has an output power loss of 33%, while the drop in the output power of the reference module was 21.8%.

Table 1 Summary of the electrical parameters of the tested PV modules

PV Module	$Voc\ (V)$ Before PID	$Voc\ (V)$ After PID	$Isc\ (A)$ Before PID	$Isc\ (A)$ After PID	$Pmax\ (W)$ Before PID	$Pmax\ (W)$ After PID
Reference Module, crack free	36.6	36.2	8.1	8.1	219.2	171.4
PV #1	36.6	35.8	8.1	8.1	217.7	161.9
PV #2	36.6	35.6	8.1	8.0	217.4	154.9
PV #3	36.5	34.4	8.1	8.0	216.2	146.8
PV #4	36.6	35.8	8.1	8.1	217.6	159.5

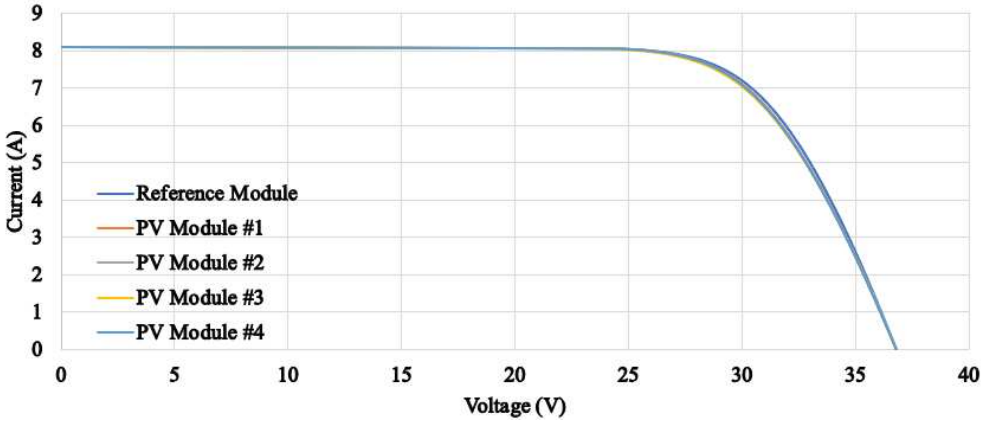

(a)

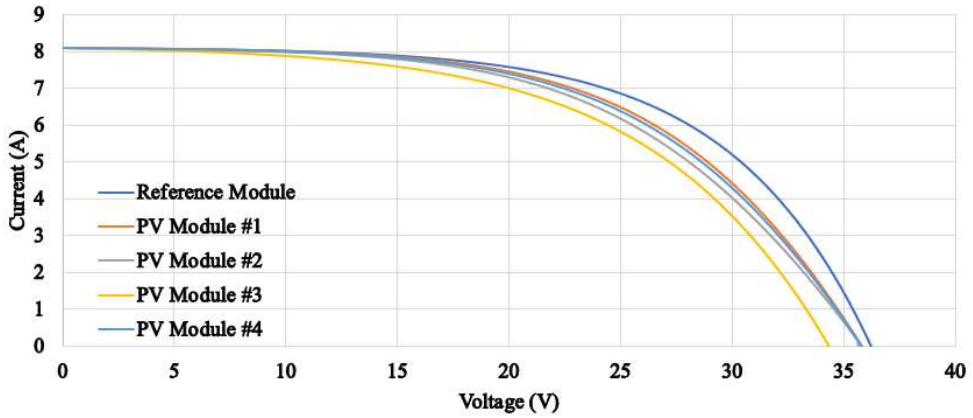

(b)

Figure 13. Comparing the output power loss before and after the PID test. (a) I-V before PID test, (b) I-V after PID test.

According to the other electrical parameters, there were no significant changes before the PID test was performed in the short circuit current and V_{oc}. After the PID experiment was completed, there was an insignificant drop in the short circuit current; however, the V_{oc} has dropped in the range of 1.1% to 4.9%. This demonstrates the significance of having cracks in PV modules. Therefore, over time, the cracks will lead to a drastic drop in output power production, and they are also plausible, compared with healthy PV modules, and they accelerate the degradation if the modules were affected by PID.

5. Conclusions

This paper reports the reliability of 186 PV modules from the production to the installation stage. Initially, no cracks or hotspots for the PV modules were found after being assembled. However, a minor reduction in the output power, ±0.3% was observed. The PV modules were delivered using standard practice, and no further precautions were considered. The EL images of all PV modules were taken at the installation site, 2.2% evolved cracks were discovered. Depending on the crack size, the estimated output power losses under STC conditions varied from 0.53% to 1.43%.

To allow hotspots to develop, the cracked PV modules had thermal images taken after being under operation for 6-months. As a result, it was observed that PV hotspots developed in all cracked PV modules and their temperature varied from 35 to 45°C. The cracked PV modules were dismounted from the PV installation, and a PID test was performed. From these tests it was discovered that the difference in the output power loss reached 10.9% after the PID test was completed, compared with 1.29% before the PID test.

These results suggest that improving the current standards for packaging and delivering PV modules must be documented. In addition, these investigations explain that the reliability of PV modules can be severely impaired if the PV modules are affected by any form of cracking modes, including micro-cracks or breakdown regions.

CRediT Authorship Contribution Statement

Mahmoud Dhimish: Formal Analysis, Methodology, Visualization, Conceptualization, Writing – original draft. **Ameer Ahmad:** Software, Validation, Visualization, Writing – review and editing. **Andy M. Tyrrell:** Validation, Funding Acquisition, Resources, Writing – review and editing.

Declaration of Competing Interest

The authors declare that they have no known competing financial interests or personal relationships that could have appeared to influence the work reported in this paper.

References

[1] Carolus, J., Tsanakas, J. A., van der Heide, A., Voroshazi, E., De Ceuninck, W., & Daenen, M. (2019). Physics of potential-induced degradation in bifacial p-PERC solar cells. *Solar Energy Materials and Solar Cells*, *200*, 109950. https://doi.org/10.1016/j.solmat.2019.109950

[2] Zhang, J. W., Cao, D. K., Diaham, S., Zhang, X., Yin, X. Q., & Wang, Q. (2019). Research on potential induced degradation (PID) of polymeric backsheet in PV modules after salt-mist exposure. *Solar Energy*, *188*, 475-482. https://doi.org/10.1016/j.solener.2019.06.019

[3] Review on Infrared and Electroluminescence Imaging for PV Field Applications. Retrieved from: https://iea-pvps.org/wp-content/uploads/2020/01/Review_on_IR_and_EL_Imaging_for_PV_Field_Applications_by_Task_13.pdf

[4] Dhimish, M. (2020). Micro cracks distribution and power degradation of polycrystalline solar cells wafer: Observations constructed from the analysis of 4000 samples. *Renewable Energy*, *145*, 466-477. https://doi.org/10.1016/j.renene.2019.06.057

[5] Qian, X., Li, J., Cao, J., Wu, Y., & Wang, W. (2020). Micro-cracks detection of solar cells surface via combining short-term and long-term deep features. *Neural Networks*, *127*, 132-140. https://doi.org/10.1016/j.neunet.2020.04.012

[6] Wang, H., Zhao, P., Yang, H., Chang, J., Song, D., & Sang, S. (2018). Performance variation of dark current density-voltage characteristics for PID-affected monocrystalline silicon solar modules from the field. *Microelectronics Reliability*, *81*, 320-327. https://doi.org/10.1016/j.microrel.2017.11.003

[7] Sporleder, K., Turek, M., Schüler, N., Naumann, V., Hevisov, D., Pöblau, C., ... & Hagendorf, C. (2021). Quick test for reversible and irreversible PID of bifacial PERC solar cells. *Solar Energy Materials and Solar Cells*, *219*, 110755. https://doi.org/10.1016/j.solmat.2020.110755

[8] Akram, M. W., Li, G., Jin, Y., Zhu, C., Javaid, A., Akram, M. Z., & Khan, M. U. (2020). Study of manufacturing and hotspot formation in cut cell and full cell PV modules. *Solar Energy*, *203*, 247-259. https://doi.org/10.1016/j.solener.2020.04.052

[9] Carolus, J., Breugelmans, R., Tsanakas, J. A., van der Heide, A., Voroshazi, E., De Ceuninck, W., & Daenen, M. (2020). Why and how to adapt PID testing for bifacial PV modules?. *Progress in Photovoltaics: Research and Applications*, *28*(10), 1045-1053. https://doi.org/10.1002/pip.3311

[10] Dhimish, M., Hu, Y., Schofield, N., & G Vieira, R. (2020). Mitigating Potential-Induced Degradation (PID) Using SiO2 ARC Layer. *Energies*, *13*(19), 5139. https://doi.org/10.3390/en13195139

[11] Sertel, T., Ozen, Y., Baran, V., & Ozcelik, S. (2019). Effect of single-layer Ta2O5 and double-layer SiO2/Ta2O5 anti-reflective coatings on GaInP/GaAs/Ge triple-junction solar cell performance. *Journal of Alloys and Compounds*, *806*, 439-450. https://doi.org/10.1016/j.jallcom.2019.07.257

[12] Wang, J., Ge, J., Hou, H., Wang, M., Liu, G., Qiao, G., & Wang, Y. (2017). Design and sol–gel preparation of SiO2/TiO2 and SiO2/SnO2/SiO2–SnO2 multilayer antireflective coatings. *Applied Surface Science*, *422*, 970-974. https://doi.org/10.1016/j.apsusc.2017.06.133

[13] Papargyri, L., Theristis, M., Kubicek, B., Krametz, T., Mayr, C., Papanastasiou, P., & Georghiou, G. E. (2020). Modelling and experimental investigations of microcracks in crystalline silicon photovoltaics: A review. *Renewable Energy*, *145*, 2387-2408. https://doi.org/10.1016/j.renene.2019.07.138

[14] Dhimish, M., d'Alessandro, V., & Daliento, S. (2021). Investigating the Impact of Cracks on Solar Cells Performance: Analysis based on Nonuniform and Uniform Crack Distributions. *IEEE Transactions on Industrial Informatics*. http://doi.org/10.1109/TII.2021.3088721

[15] Olalla, C., Hasan, M., Deline, C., & Maksimović, D. (2018). Mitigation of hot-spots in photovoltaic systems using distributed power electronics. *Energies*, *11*(4), 726. https://doi.org/10.3390/en11040726

[16] Dhimish, M., & Badran, G. (2020). Current limiter circuit to avoid photovoltaic mismatch conditions including hot-spots and shading. *Renewable Energy*, *145*, 2201-2216. https://doi.org/10.1016/j.renene.2019.07.156

[17] Tang, S., Xing, Y., Chen, L., Song, X., & Yao, F. (2021). Review and a novel strategy for mitigating hot spot of PV panels. *Solar Energy*, *214*, 51-61. https://doi.org/10.1016/j.solener.2020.11.047

[18] Rajput, A. S., Ho, J. W., Zhang, Y., Nalluri, S., & Aberle, A. G. (2018). Quantitative estimation of electrical performance parameters of individual solar cells in silicon photovoltaic modules using electroluminescence imaging. *Solar Energy*, *173*, 201-208. https://doi.org/10.1016/j.solener.2018.07.046

[19] Akram, M. W., Li, G., Jin, Y., Chen, X., Zhu, C., Zhao, X., ... & Ahmad, A. (2019). CNN based automatic detection of photovoltaic cell defects in electroluminescence images. *Energy*, *189*, 116319. https://doi.org/10.1016/j.energy.2019.116319

[20] Islam, M. A., Hasanuzzaman, M., & Abd Rahim, N. (2018). A comparative investigation on in-situ and laboratory standard test of the potential induced degradation of crystalline silicon photovoltaic modules. *Renewable Energy*, *127*, 102-113. https://doi.org/10.1016/j.renene.2018.04.051

[21] Zhang, J. W., Cao, D. K., Cui, Y. C., Wang, F., Putson, C., & Song, C. (2019). Influence of potential induced degradation phenomena on electrical insulating backsheet in photovoltaic modules. *Journal of Cleaner Production*, *208*, 333-339. https://doi.org/10.1016/j.jclepro.2018.10.057

[22] Oh, W., Bae, S., Chan, S. I., Lee, H. S., Kim, D., & Park, N. (2017). Field degradation prediction of potential induced degradation of the crystalline silicon photovoltaic modules based on accelerated test and climatic data. *Microelectronics Reliability*, *76*, 596-600. https://doi.org/10.1016/j.microrel.2017.07.079

[23] Dhimish, M., Holmes, V., Mehrdadi, B., Dales, M., & Mather, P. (2018). PV output power enhancement using two mitigation techniques for hot spots and partially shaded solar cells. *Electric Power Systems Research*, *158*, 15-25. https://doi.org/10.1016/j.epsr.2018.01.002

[24] Mirtchev, A., Mouselinos, T., Syrigos, S., & Tatakis, E. (2021). Behavioral Analysis of Potential Induced Degradation on Photovoltaic Cells, Regeneration and Artificial Creation. *Energies*, *14*(13), 3899. https://doi.org/10.3390/en14133899

[25] Luo, W., Khoo, Y. S., Hacke, P., Naumann, V., Lausch, D., Harvey, S. P., ... & Ramakrishna, S. (2017). Potential-induced degradation in photovoltaic modules: a critical review. *Energy & environmental science*, *10*(1), 43-68. http://doi.org/0.1039/C6EE02271E

[26] Sulas-Kern, D.B. et al. Electrochemical degradation modes in bifacial silicon photovoltaic modules. Prog. Photovolt. 1-11 (2021). https://doi.org/10.1002/pip.3530

[27] Dhimish, M. & Lazaridis, P. I.. An empirical investigation on the correlation between solar cell cracks and hotspots. *Scientific Reports.* 11, 23961 (2021). https://doi.org/10.1038/s41598-021-03498-z

[28] Dhimish, M. & Kettle, J. Impact of Solar Cell Cracks Caused During Potential-Induced Degradation (PID) Tests. *IEEE Trans. Electron Devices.* 69, 604-612 (2021). http://doi.org/10.1109/TED.2021.3135365

[29] Carolus, J. *et al*. Physics of potential-induced degradation in bifacial p-PERC solar cells. *Sol. Energy Mater. Sol. Cells* 200, 109950 (2019). http://doi.org/10.1016/j.solmat.2019.109950

[30] Dhimish, M. & Tyrrell, A.M. Power loss and hotspot analysis for photovoltaic modules affected by potential induced degradation. *NPJ Mater. Degrad.* 6, 1-8 (2022). http://doi.org/10.1038/s41529-022-00221-9

[31] Bedrich, K.G. *et al*. Quantitative electroluminescence imaging analysis for performance estimation of PID-influenced PV modules. *IEEE J. Photovolt.* 8, 1281-1288 (2018). DOI: http://doi.org/10.1109/JPHOTOV.2018.2846665

[32] Dhimish, M., & Badran, G. Recovery of Photovoltaic Potential-Induced Degradation Utilizing Automatic Indirect Voltage Source. *IEEE Transactions on Instrumentation and Measurement*. 71, (2021). DOI: http://doi.org/10.1109/TIM.2021.3134328